Chemical Engineering Science 77 (2012) 47–56

Contents lists available at SciVerse ScienceDirect

Chemical Engineering Science

journal homepage: www.elsevier.com/locate/ces

Synthesis, crystallization and characterization of diastereomeric salts formed by ephedrine and malic acid in water

Han Wu [a,*], Anthony R. West [b], Martin Vickers [c], David C. Apperley [d], Alan G. Jones [a,*]

[a] Department of Chemical Engineering, UCL, Torrington Place, London WC1E 7JE, UK
[b] Department of Materials Science and Engineering, University of Sheffield, Sheffield S1 3JD, UK
[c] Department of Chemistry, UCL, 20 Gordon Street, London WC1H 0AJ, UK
[d] Department of Chemistry, Durham University, South Road, Durham DH1 3LE, UK

ARTICLE INFO

Article history:
Received 6 October 2011
Received in revised form
28 November 2011
Accepted 6 December 2011
Available online 16 December 2011

Keywords:
Crystallization
Chiral separation
Ephedrine salts
Hydrates
X-ray diffraction

ABSTRACT

A screening of crystallization conditions for the diastereomeric salts formed by L/D-malic acid and a common resolving agent, L-Ephedrine, in water is reported. So far, 7 different forms of salts with 1:1 and 2:1 stoichiometries were successfully crystallized, including one previously reported 1:1 LL salt. All new salts were characterized by differential scanning calorimetry, thermogravimetric and elemental analysis, infrared spectroscopy, solid-state NMR and powder XRD. 1:1 stoichiometry favours anhydrate formation while 2:1 stoichiometry tends to give monohydrate forms. Two monohydrates dehydrate on heating to produce anhydrous salts. A 2:1 LD trihydrate was discovered by vapor sorption experiments and is stable only at high relative humidity (> 50%).

Differences in stoichiometry and hydrate formation during salt crystallization, leading to differences in physicochemical properties could have a significant impact on resolution conditions and outcome.
© 2011 Elsevier Ltd. All rights reserved.

1. Introduction

Chiral resolution via crystallization is of great importance for the food and pharmaceutical industries due to different pharmacological effects (i.e. inactive, toxic or side effects) of enantiomers and the racemic mixture (Vermeulen and te Koppele, 1993). For this reason, the American Food and Drug Administration (FDA) introduced a new regulatory guideline for identification and quantification of pharmacological/toxicological effects of chiral drugs, and the strict production of enantiopure forms. Many separation techniques such as chiral chromatography, enantioselective membrane separation and spontaneous or preferential crystallization have been developed to achieve chiral resolution but have limited applications in industry due to various problems such as scale-up, cost-effectiveness and restricted application to conglomerate forming systems. Therefore, classical resolution via formation of diastereomeric salt pairs and precipitation of the least soluble salts (Kozma, 2001) remains one of the most widely used methods to produce optically pure enantiomers at moderate cost, and is particularly amenable to scale-up.

Unlike enantiomers whose crystal structures and physical properties are identical, most diastereomeric salts can be separated by crystallization due to their large solubility difference (Jacques et al., 1981; Anandamanoharan et al., 2006). In addition, these salts may exhibit different crystal morphology, thermal stability (melting point and melting enthalpy), processability, dissolution rate, hygroscopicity and unequal tendency to crystallize. Such salt pairs (regarded as intermediates during chiral resolution processes) could therefore be advantageous compared to the corresponding free acid or base. It is estimated that more than 50% of drugs used in medicine are administered as salts (Stahl and Wermuth, 2002). Exploration of salt forms is therefore of both scientific and commercial interest.

L-Ephedrine (L-Eph) is an active drug ingredient extracted from the herb Ephedra sinica (Ma Huang). It has been widely used as an appetite depressant, bronchodilator agent, central nervous system stimulant and treatment for cold, flu, and asthma (Abourashed et al., 2003). It is best known as a dietary supplement for promoting weight loss, increasing body energy and enhancing athletic performance. However, L-Eph free form has many undesired properties such as low thermal/thermodynamic stability and high hygroscopicity, revealed by its low melting point and quick rehydration in air. This motivates us to establish new possible L-Eph salt systems.

The first aim of this study is to screen a family of salt pairs using a common chiral base, L-(1R, 2S)-(−)-Ephedrine, Fig. 1a,

* Corresponding authors. Tel.: +44 20 7679 3828; fax: +44 20 7383 2348.
E-mail addresses: han.wu@ucl.ac.uk, hanwu03@hotmail.com (H. Wu), a.jones@ucl.ac.uk (A.G. Jones).

0009-2509/$ - see front matter © 2011 Elsevier Ltd. All rights reserved.
doi:10.1016/j.ces.2011.12.007

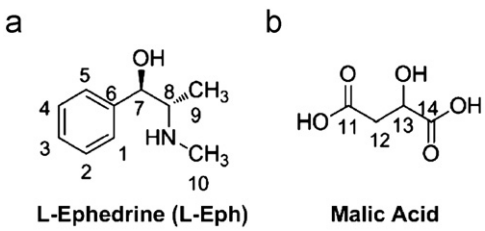

Fig. 1. Chemical structure of (a) L-Ephedrine (L-Eph) and (b) malic acid.

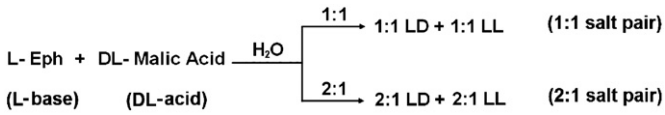

Fig. 2. Schematic route to formation of 1:1 and 2:1 salt pairs by resolving agents L-Eph and DL-malic acid in water. LL=L-Eph L-malate, LD=L-Eph D-malate.

to react with racemic DL-(±)-malic acid, Fig. 1b, in water. Only one salt, 1:1 L-Eph L-malate (1:1 LL), has been reported for this system (Collier et al., 2006), but in theory, four salts with 1:1 and 2:1 stoichiometry could form by acid–base reaction, due to the dibasic nature of malic acid (Fig. 2).

Organic pharmaceuticals often exhibit different crystalline forms, e.g. variable stoichiometry, polymorphs, hydrates and solvates (Van de Streek, 2007; Wu et al., 2010a, 2010b; Wu and West, 2011), which makes it challenging and exhaustive to predict the phases and synthesis conditions of relevant crystal forms during salt formation. To tackle this problem, experimental input is needed to crystallize and identify each phase-pure salt, monitor possible phase transitions between different salts, analyze their physiochemical properties and compare their relative stability. In reality, such information is sparsely available in the literature.

This motivates the second objective of this study, which is to provide a dataset of the physicochemical properties of the resulting L-Eph salt pairs. Such a dataset could be used as a prelude to solubility and resolution studies.

The present work concerns: (i) synthesis and crystallization of 2 pairs (1:1 and 2:1 stoichiometry) of possible salts from L-Eph and racemic DL-malic acid; (ii) study of hydrate formation, thermal stability and polymorphism; (iii) screening of salt formation conditions and (iv) determination of preliminary structural and thermodynamic data as a prelude to resolution tests.

2. Experimental

2.1. Materials

L- (≥ 99.5%), D- (≥ 97.0%) and DL-malic acids (≥ 99.0%): Sigma Aldrich; L-Eph (99.0–101.0%): Acros Organic, Thermo Fisher Scentific. HPLC-grade solvents were used for crystallization experiments. L-Eph has a tendency to hydrate under ambient conditions and was stored in a refrigerator. Both hydrated and anhydrous forms of L-Eph melt at ~37 ± 1 °C (Cooke et al., 2010). All materials were used, as received, without further purification. A small amount of hydrated phase was found in L-Eph by powder X-ray diffraction.

2.2. Preparation of salt forms

Stoichiometric (1:1 and 2:1) L-Eph malates were crystallized by cooling or slow evaporation from saturated solution at room temperature (Black et al., 2007). Crystalline material was separated out using a 0.45 μm pore membrane filter and dried at 30 °C for 48 h. However, attempts to grow single crystals for structure determination failed, producing either twinned crystals or amorphous material. Mechanical grinding has been used recently to produce salts or co-crystals from solid mixtures and usually the most stable form is obtained under mechanical stress. We applied this method to examine the formation of L-Eph salts by milling stoichiometric mixtures of L-Eph and malic acid in a pestle and mortar for 10 min, with and without one droplet of water (ca. 10 μL). Salts grown from saturated solution were also ground to check their stability.

2.3. Characterization

Powder X-ray Diffraction (XRD). Routine phase characterization used a STOE STADI-P powder X-ray diffractometer (Cu $K\alpha_1$ radiation, λ=1.5406 Å), equipped with a Ge (111) monochromator and linear position sensitive detector (PSD) in Debye–Scherrer geometry. Samples were prepared in 0.6 mm borosilicate glass capillaries and aligned on a rotating goniometer head for measurements over the 2θ range 2–45°. PXRD patterns of the pure salt forms were indexed using CRYSTFIRE (Shirley, 1980); the space group was determined by statistical assessment of systematic absences and the unit cell was refined by Le Bail whole pattern fitting.

Thermal analysis. DSC experiments were performed using two different instruments, a Perkin-Elmer Diamond DSC equipped with an Intracooler 2P cooling system under dry N_2 and a Perkin Elmer DSC 6 under dry Ar. Diamond DSC was calibrated for temperature with pure In (purity 99.999%, mp 156.6 °C) and benzophenone (recrystallized from 2-propanol, mp 48 °C); DSC 6 was calibrated with pure In and Zn (purity 99.999%, mp 419.5 °C). The heat flow for both instruments was calibrated using In (ΔH=28.45 J/g). Pyris 7.0 software was used for data analysis. Approximately 5–8 mg sample was weighed into an Al pan fitted with a perforated lid, and analyzed at a heating/cooling rate of 10 °C/min. The weight loss as a function of temperature was determined by Thermogravimetric Analysis, TGA, using a Perkin Elmer Pyris 1 TG system, at a heating rate of 10 °C/min in dry N_2.

Elemental analysis. Elemental compositions of identified pure salt forms were determined by an Exeter Analytical CE-440 Elemental Analyzer using a thermal conductivity detection method for measuring C, H and O contents in salts after combustion and reduction.

Attenuated Total Reflection Fourier Transform Infrared Spectroscopy (ATR–FTIR). The IR spectra of solid forms of pure salts were collected using a Perkin Elmer Spectrum One FTIR spectrometer with ATR sampling technique. All spectra were collected between 4000 and 650 cm^{-1} at a resolution of 4 cm^{-1}. 12 scans were accumulated for each spectrum to increase signal to noise ratio. Perkin Elmer Spectrum software was used for data analysis.

Dynamic Vapor Sorption (DVS). Moisture sorption isotherms at 25 °C of salts were conducted to check their reaction to humidity change using a Surface Measurement Systems DVS automated water sorption analyzer, integrated with DVSWin software, version 2.17. About 10–15 mg of solid was placed in the analyzer and mass change monitored while relative humidity (RH) was varied between 0% and 95% at intervals of 10% RH. Each step was held until a stable mass had been achieved.

Solid State Nuclear Magnetic Resonance (SS NMR). Spectra were recorded using a Varian VNMRS 400 spectrometer operating at 100.56 MHz for ^{13}C with a 6 mm T3 HXY probe operating in double resonance mode. High-resolution data were obtained under magic-angle spinning (MAS) conditions using cross-polarization (CP) experiment. The CP mode was performed at a recycle

rate of 7.5 s, contact time of 1 ms and a MAS rate of 6.8 kHz. Spectra were referenced to tetramethylsilane by setting the high-frequency signal from adamantane to 38.5 ppm.

3. Results and discussion

3.1. Crystallization of 1:1 and 2:1 salt pairs

Three methods were used for salt formation: solution crystallization (cooling crystallization and solvent evaporation), grinding crystallization (solvent-free and solvent-assisted grinding) and phase alternation in a RH-controlled box. In total, seven different solid forms were crystallized: 4 grown from solution and 3 grown under various RH (Fig. 3). Full characterization of the products by XRD, SS NMR, FT-IR, DSC/TGA and elemental analysis confirmed the formation of new crystalline phases, including unambiguous identification of 7 salts from their XRD patterns.

Solution crystallization. Routine crystallizations by cooling or evaporation of a saturated aqueous solution were performed for an initial screen of salt formation. Four different high-crystallinity salts: 1:1 LL, 1:1 LD, 2:1 LL_MH and 2:1 LD_TH were successfully produced. Solution crystallization of phase-pure 1:1 salts is very slow and difficult: cooling crystallization of saturated solution failed to produce a crystalline solid of 1:1 LL or 1:1 LD salt instead, a highly-viscous yellow solution was formed: Slow evaporation leads to formation of yellow oil, which then converted slowly to a crystalline phase after ~1 month. Mechanical disturbance by a spatula was found to induce nucleation and provided a useful method to increase the rate of conversion to crystalline solid. The observed crystallization behavior indicated the high aqueous solubility of the 1:1 salt pair and a large metastable zone width, which could cause handling issues due to its highly viscous nature in water and potential difficulties in solubility analysis.

Solution crystallization of the phase-pure 2:1 MH salt pair as a monohydrate phase was successful and reproducible. However, DVS analysis of 2:1 LD_MH under various RH suggested the existence of a trihydrate form, which could be more stable and need a longer time for crystallization. Therefore, the solids crystallizing from saturated solution at various times were re-examined: from the immediate occurrence of crystallization until the solution had been further mixed for 1 week; all samples collected were confirmed to be 2:1 LD_TH rather than MH form, indicating this TH form to be kinetically and thermodynamically most favorable at room temperature. This raises the question of the stability of 2:1 LD_TH salt in the dry state. A careful check of the powders during filtration and drying confirmed that TH was slowly converted to MH in a dry atmosphere. Once a solid sample of 2:1 LD_MH is obtained, either by dehydration of TH or hydration of anhydrate, it is stable indefinitely in air (< 40% RH).

Grinding crystallization. As an alternative crystallization method, grinding is effective for crystallization of multi-component systems such as co-crystals (Chadwick et al., 2007). This technique was applied both to confirm salt formation and as an attempt to produce bulk samples of 1:1 LL and 1:1 LD salts. Both solvent-free (dry grinding) and solvent-assisted (wet grinding) grinding were employed: different stoichiometric mixtures of L-Eph and malic acid (1:1 and 2:1) were ground in a mortar and pestle for 10 min, with or without one droplet of H_2O (ca. 10 μL). All ground samples were analyzed by IR, XRD and elemental analysis to confirm successful salt formation. Crystallization results are summarized in Table 1.

Grinding a 1:1 mixture leads to formation of a viscous melt or gel. Subsequent crystallization requires extra drying at room

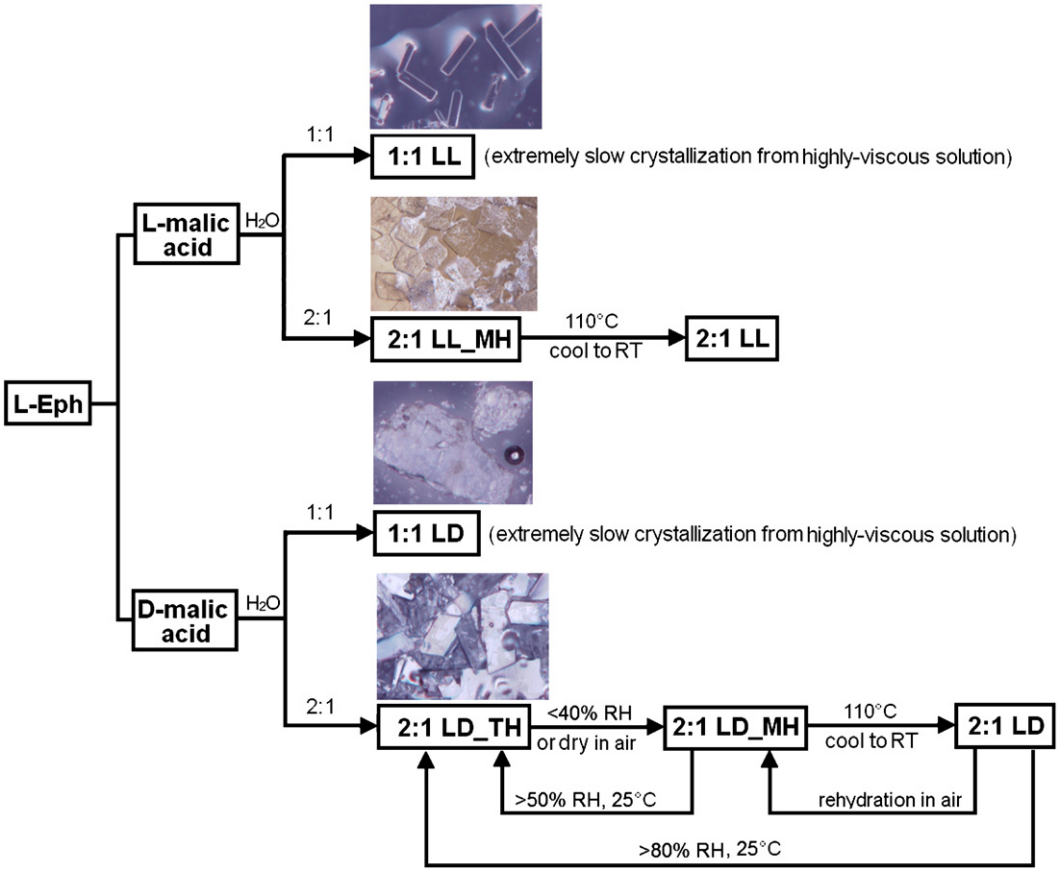

Fig. 3. Overview of salt formation in the system L-Eph–Malic acid–H_2O; MH = monohydrate, TH = trihydrate.

temperature. This is particularly advantageous for formation of 1:1 LL salt: ground powders showed higher crystallinity, higher purity and uniform crystal size compared to solution-grown samples. Grinding results from the 2:1 stoichiometry were also superior, offering significant reduction of crystallization time, processing steps and sample loss compared to the traditional solution method. Both dry and wet grinding of 2:1 LD mixture tends to produce MH form, providing a direct way to obtain this salt. Possibly, dry grinding produces the anhydrous form first, which then quickly transforms to the hydrate, absorbing moisture from the air. Alternatively, moisture from the air may be incorporated during salt formation. To test this, rapid IR analysis requiring only a few seconds was carried out and showed no trace of the anhydrous phase. The grinding result of 2:1 LD_MH, consistent with high purity, is different from the solution crystallization result (producing 2:1 LD_TH), and indicates that monohydrate is the most stable form thermodynamically under ambient conditions. Dry grinding of 2:1 LL showed the formation of a new salt, mixed with other phases. Full characterization of this new salt has not yet been achieved due to the difficulty in obtaining it in a pure form.

The addition of one drop of water during grinding not only accelerates the process of salt formation, but also gives more reproducible results with high-purity salt forms (e.g. dry grinding of 1:1 L-Eph with D-Malic acid sometimes produces a mixture of 2:1 LD_MH and unknown phases due to poor mixing, while wet grinding of the same materials always yields pure 1:1 LD salt). The role of the solvent in grinding is not fully understood but could be related to (i) better mixing provided by the solvent droplet acting as a lubricant, (ii) enhanced dissolution rate of the reactants, (iii) formation of intermediate/permanent solvate phases. In summary, our results demonstrated that grinding crystallization, especially solvent-assisted grinding, is more efficient than crystallization from solution, and provides a simple, reproducible and appropriate method to produce high-purity, maximum-yield, microcrystalline salts without involvement of lengthy dissolution, nucleation, crystal growth, filtration, purification and drying processes.

Table 1
Crystallization results from dry and wet grinding of stoichiometric mixtures of L-Eph and malic acid powders.

	L-Eph+L-malic acid		L-Eph+D-malic acid	
Stoichiometry	1:1	2:1	1:1	2:1
Dry grinding	1:1 LL salt	Multi-phases	1:1 LD salt	2:1 LD_MH salt
Wet grinding	1:1 LL salt	2:1 LL_MH salt	1:1 LD salt	2:1 LD_MH salt

RH-controlled crystallization. As discussed above, solution and grinding methods failed to produce any 2:1 anhydrous phases reproducibly, so a third method, controlling RH and temperature, was applied. Pure anhydrous phases of 2:1 LL and 2:1 LD salts were obtained by dehydration of corresponding hydrates in desiccators (P_2O_5 as drying agent) at 70 °C in an oven. With high RH, as revealed later by DVS analysis, 2:1 LD_TH salt was obtained from the MH form at 50% RH and from the anhydrous form at 80% RH at room temperature. 2:1 LD_MH was produced by dehydration of TH at 40% RH and was stable over the RH range 0–40% at room temperature.

3.2. Characterization of salt pairs by XRD

The crystallized salt pairs were characterized by powder XRD. The only salt known from the literature, 1:1 LL, was reproduced by solution and grinding crystallization: its XRD pattern matches well the powder pattern simulated from single crystal data (Fig. 4). XRD patterns of the 7 salts are distinctive, with sharp, characteristic peaks for each phase, indicating the formation of high-purity crystalline solid phases, in agreement with the elemental analysis, shown in Table 2. This is further supported by satisfactory indexing and unit cell refinement of XRD data (Table 3). As an example, the Le Bail whole pattern fit for the 1:1 LD salt (Fig. 5) is excellent, suggesting that such material is indeed single phase.

The next step is to determine the crystal structures for each salt pair, calculate their lattice energy differences and correlate these with their relative stabilities. Although suitable single crystals are not yet available, the lattice energy and relative stability of salt pairs may be inferred from density inequalities: the unit cell data show that the LL salts are more densely packed compared to their LD analogs (Table 3), which might indicate that

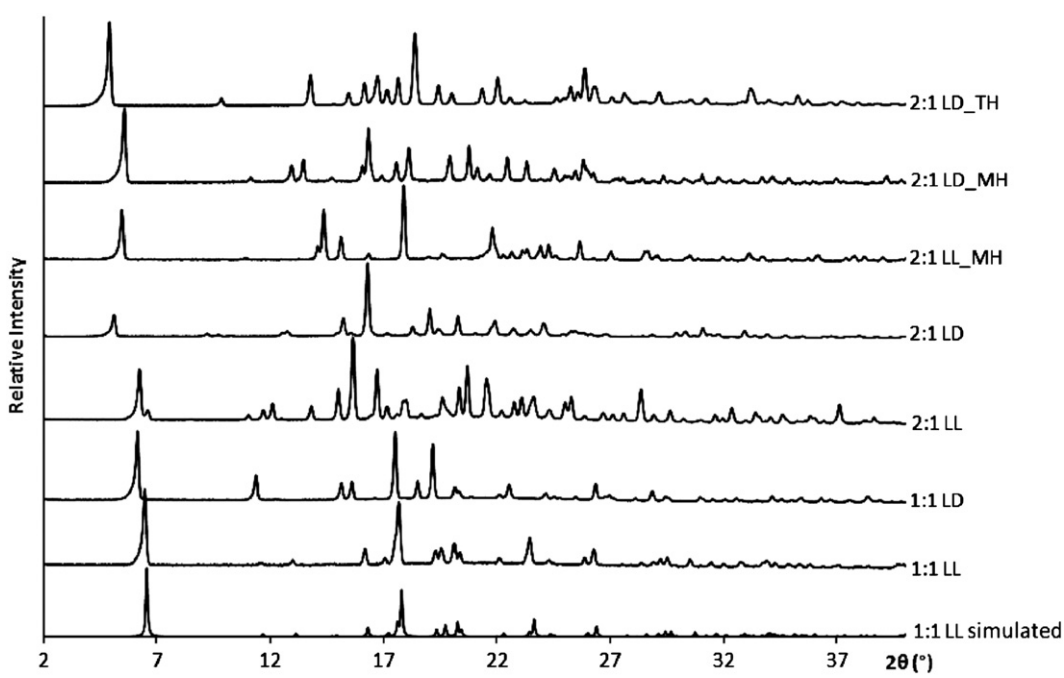

Fig. 4. Powder XRD patterns of seven phase—pure 1:1 and 2:1 salt forms, $\lambda = 1.5406$ Å.

Table 2
Elemental analysis of solid salt forms.

	1:1			2:1			2:1_MH			2:1_TH	
	Calculated	1:1 LL	1:1 LD	Calculated	2:1 LL	2:1 LD	Calculated	2:1 LL_MH	2:1 LD_MH	Calculated	2:1 LD_TH
C	56.17	56.78	55.79	62.07	62.17	61.73	59.75	59.87	59.67	55.49	54.08
H	7.07	7.26	7.06	7.76	7.88	7.89	7.88	8.03	7.97	8.29	7.40
N	4.68	4.70	4.64	6.03	6.03	5.91	5.81	5.79	5.77	5.39	5.15

Table 3
Crystallographic data of salts determined from powder XRD.

	1:1 Salt pair		2:1 Salt pair		2:1_MH Salt pair		2:1_TH
	1:1 LL[a]	1:1 LD	2:1 LL	2:1 LD	2:1 LL_MH	2:1 LD_MH	2:1 LD_TH
Formula	$C_{10}H_{16}NO$ $C_4H_5O_5$	$C_{10}H_{16}NO$ $C_4H_5O_5$	$(C_{10}H_{16}NO)_2$ $C_4H_4O_5$	$(C_{10}H_{16}NO)_2$ $C_4H_4O_5$	$(C_{10}H_{16}NO)_2$ $C_4H_4O_5 \cdot H_2O$	$(C_{10}H_{16}NO)_2$ $C_4H_4O_5 \cdot H_2O$	$(C_{10}H_{16}NO)_2$ $C_4H_4O_5 \cdot (H_2O)_3$
Formula weight	299.3	299.3	464.6	464.6	482.6	482.6	518.6
Lattice system	Monoclinic	Monoclinic	Monoclinic	Monoclinic	Orthorhombic	Triclinic	Triclinic
Space group	$P2_1$	$P2_1$	$P2_1$	$P2_1$	$P2_12_12_1$	P1	P1
a **(Å)**	6.131 (1)	14.482 (2)	15.105 (1)	17.490 (1)	32.212 (2)	7.314 (1)	5.985 (1)
b **(Å)**	9.172 (1)	9.247 (1)	28.217 (2)	7.564 (1)	9.413 (1)	16.052 (1)	7.112 (1)
c **(Å)**	13.739 (2)	6.093 (1)	5.763 (1)	9.736 (1)	8.409 (1)	5.825 (1)	18.195 (1)
α (deg.)	90.000	90.000	90.000	90.000	90.000	96.459 (1)	99.738 (2)
β (deg.)	100.909 (4)	97.442 (10)	90.141 (10)	100.200 (3)	90.000	109.799 (1)	91.015 (3)
γ (deg.)	90.000	90.000	90.000	90.000	90.000	94.325 (1)	66.369 (2)
v **(Å^3)**	758.66 (15)	809.07 (12)	2456.24 (26)	1267.60 (10)	2549.78 (32)	634.61 (36)	698.21 (84)
Density calculated (g cm^{-3})	1.310	1.228	1.256	1.217	1.257	1.263	1.233

[a] Crystallographic data of 1:1 LL were obtained from single crystal data (Collier et al., 2006).

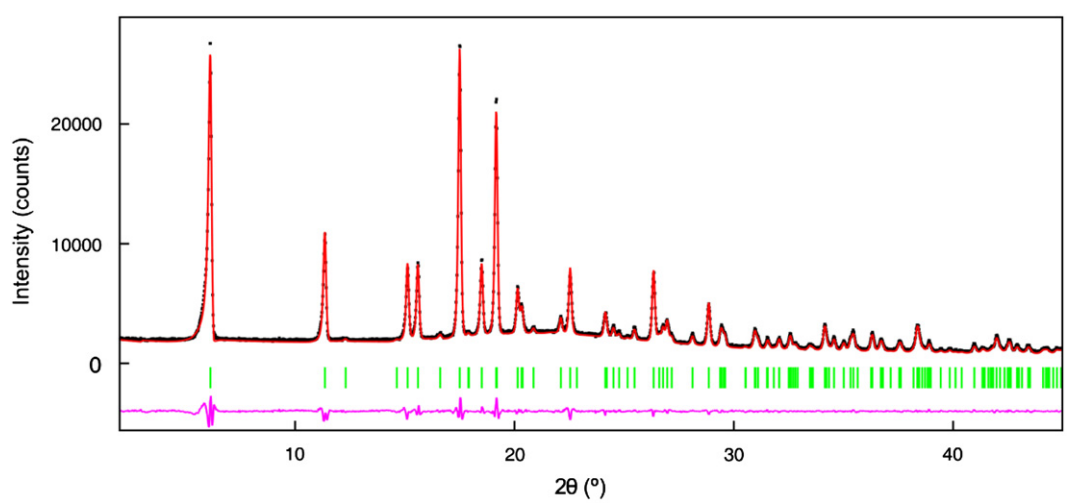

Fig. 5. Le Bail fit of 1:1 LD salt showing observed (●), calculated (–), expected (|) and difference (–) plot.

LL salts possess lower free energy and are thermodynamically more stable than the corresponding LD salts. Therefore, the separation of LL salts from the racemic solution could be feasible under suitable crystallization conditions. However, the formation of 2:1 hydrates readily in water showed comprehensive impact on the crystal structures and calculated densities, leading to more variations and unpredictability in resolution.

3.3. ^{13}C SS NMR chemical shift assignment and salt composition determination

The crystallization product of an organic compound can be very different from that expected; in particular, "salt formation as a result of proton transfer from the acid to the base frequently results in a lattice with an unpredictable chemical (solvates) or stoichiometric composition" (Aakeroy et al., 2007). Therefore, a set of solid state analytical techniques including SS NMR, ATR-FTIR and TGA/DSC was used to determine salt stoichiometry, ionization state, hydrate formation and chemical formula.

The ^{13}C SS NMR spectra of all solid forms of L-Eph salts displayed well-resolved patterns with general features of L-Eph and malic acid (Fig. 6). The chemical shift values were assigned mostly based on the solution state ^{13}C NMR data of norephedrine and L-malic acid (Spectral Database for Organic Compounds SDBS, 2011).

There are twice as many resonances in the spectrum of both L-Eph and L-malic acid crystals as expected, which is a clear indication of existence of two independent molecules in the solid

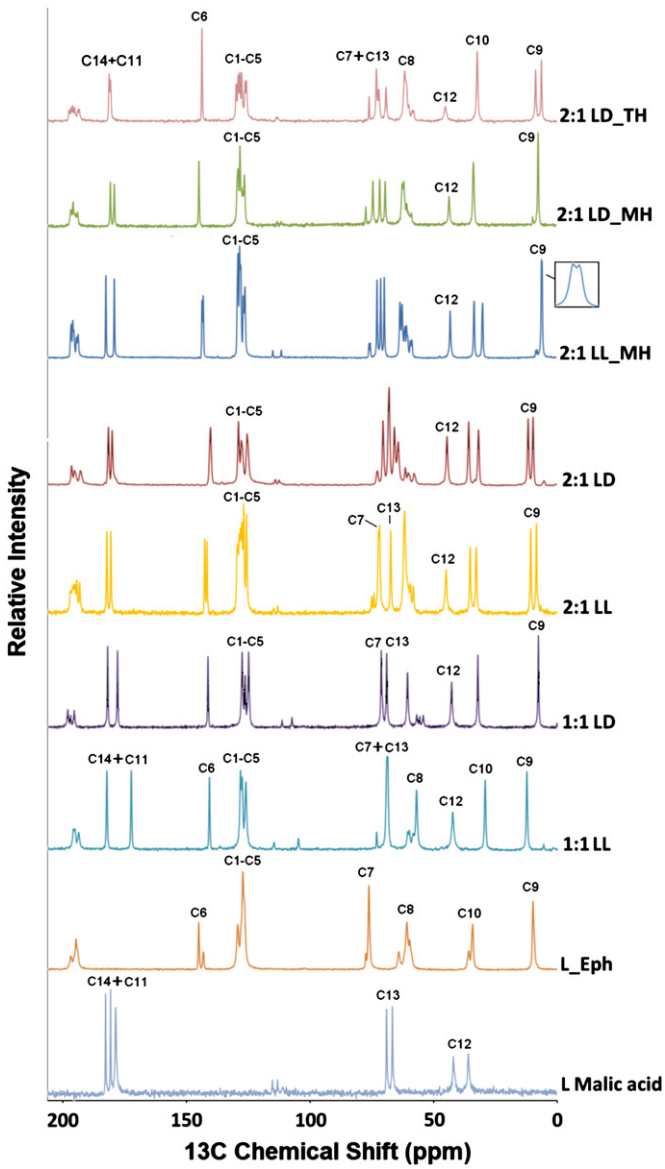

Fig. 6. ^{13}C SS NMR patterns of L-malic acid, L-Eph and seven different salt forms.

sample. This is in good agreement with our XRD analysis of both samples. The L-Eph sample is a mixture of anhydrate and hemihydrate; one unique conformation was seen from each crystal structure. The L-malic acid sample was pure and two different conformations (dimer) exist in the same crystal structure ($Z'=2$).

Significant differences in the chemical shifts were observed for seven solid salt forms, due to the number of different L-Eph molecules in the asymmetric unit (Fig. 6). For 1:1 stoichiometry, only one conformation of L-Eph was seen as three closely spaced singlets at 125–130 ppm (e.g. resonances at 124.98, 126.35 and 127.58 ppm corresponding to *m*-, *o*- and *p*-carbon, C1–C5, in 1:1 LD salt). For 2:1 salts, more complicated resonances in this region were due to the presence of two non-equivalent L-Eph molecules in the crystal structure. The only exception was 2:1 LD salt, which had three resonances, suggesting the Ar group from two L-Eph molecules was present in similar environments in the crystal lattice. The stoichiometry was confirmed by the chemical shift of the methyl carbon, C9, at 5–10 ppm: there was a singlet for 1:1 salts and two signals for 2:1 salts (except 2:1 LD_MH). The components of the spectra attributing to malic acid were much easier to identify: the carbonyl region (C11 and C14, 175–185 ppm) and methylene region (C12, 42.8–44.4 ppm) were easily recognized. The C12 environments were similar for both 1:1 and 2:1 stoichiometries with only one characteristic peak at similar chemical shift value, thereby supporting the hypothesis that there is only one conformation of malic acid molecule in the asymmetric unit for all salt forms.

The number of observed ^{13}C resonances revealed the stoichiometries of the salts to be 1:1 and 2:1, as expected. The existence of two independent acid/base molecules in the asymmetric unit for 1:1 stoichiometry and three acid/base molecules for 2:1 stoichiometry, thus confirmed $Z'=1$ (Z', the number of formula units in the asymmetric unit of crystal structure). The determination of Z' from NMR spectra could be crucial to selecting the correct unit cell from the XRD pattern, thereby providing a complementary technique in the study of different crystal forms. Reported cases where "unpredictable stoichiometry resulting from the incorporation of a free carboxylic acid into the lattice" are not rare during salt formation (Aakeroy et al., 2007), and cause a highly disruptive impact on prediction/determination of crystal structures. Our SS NMR spectra unambiguously showed that $Z'=1$, ruling out possible complications of multiple molecular arrangements in the unit cell.

SS NMR may also exhibit additional information about atomic positions because it is sensitive to differences in the chemical environment of nuclei caused by differences in their crystal structures. As an example, the overall spectra of 2:1 salts were distinguishable, (e.g. the chemical shifts of C7, C10, C11 and C14 groups affected by hydrogen bonding motifs were clearly different), indicating distinctive intra-molecular (conformation) and inter-molecular packing arrangements in the crystal lattice. However, it is very difficult to interpret chemical shifts and fully understand crystal structures of different salt forms without single crystal data.

In summary, SS NMR provided a direct recognition of salt compositions, an easy comparison of 7 different salt forms, and complementary structural information to XRD.

3.4. ATR-FTIR spectroscopic study of ionization state

As a direct check of the ionization state of the molecules and hence salt formation, solid state ATR-FTIR measurements of 7 different solid forms of L-Eph salts were compared with that of the pure acid (Fig. 7). The assignments of some characteristic absorption bands are summarized in Table 4.

The carbonyl stretching absorptions (4, 6 and 7) are the strongest IR absorptions with distinguishing characteristics for each of the solid forms and therefore can be used for phase identification. In neutral form, L-malic acid molecules were characterized by a strong single peak at 1691 cm^{-1} due to ν(C=O), labeled as 4. In di-ionized form, e.g. 2:1 salts, the ν(C=O) was missing, both carboxyl groups were deprotonated to give peaks at 6 and 7, for ν_{as}(COO$^-$) and ν_s(COO$^-$), respectively. In mono-ionized form, e.g. 1:1 salts, three peaks appeared at 4, 6 and 7, corresponding to ν(C=O), ν_{as}(COO$^-$) and ν_s(COO$^-$), respectively (Fig. 7).

The two vibrational bands of ν_{as}(COO$^-$) and ν_s(COO$^-$) confirmed the proton transfer from L-malic acid to L-Eph molecules during salt formation, in good agreement with a general $\Delta pK_a > 3$ rule ($\Delta pK_a = pK_a$ base (9.74)–pK_a acid (3.46 and 5.10) (Black et al., 2007)) in water (Childs et al., 2007). The three peaks in the carbonyl regions for 1:1 salts indicated two different carbonyl environments: one was H-bonded to give one signal at 4 and the other was ionized to appear as two peaks at 6 and 7. In many cases, overlapped bands were observed in regions 5 and 6 for both 1:1 and 2:1 salts due to the indistinguishable δ(N–H) and ν_{as}(COO$^-$) vibrations at similar energy.

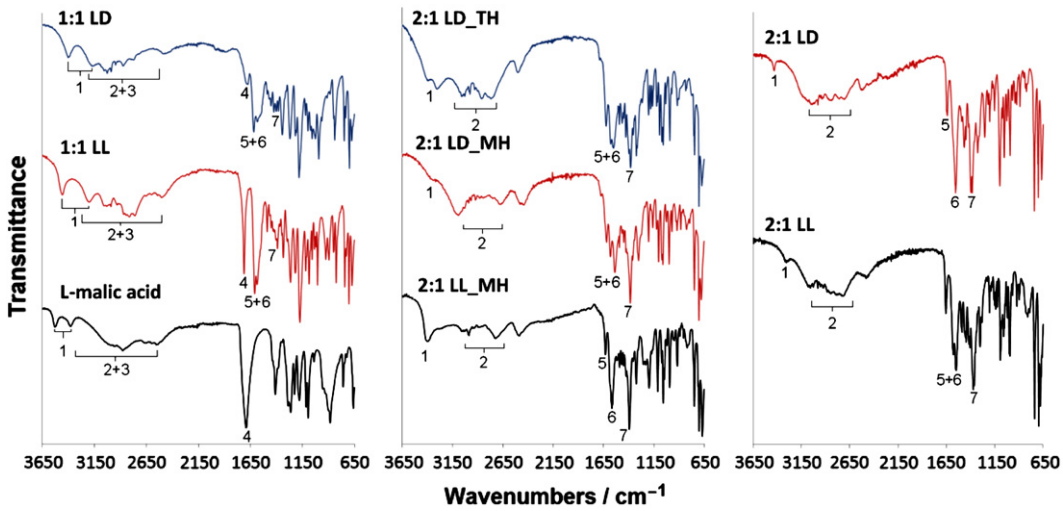

Fig. 7. ATR–FTIR spectra of L-malic acid and 7 solid forms of L-Eph salts.

Table 4
IR spectral assignments for L-malic acid and its L-Eph salts in Fig. 7.

Region number	Wavenumbers (cm^{-1})	Approximate assignments
1	3200–3645	O–H stretch (alcohol, free or H–bonded), broad
	3070–3500	N–H stretch (free or H–bonded)
2	2650–3030	C–H stretch
3	2500–3300	O–H stretch (COOH), very broad
4	1690–1760	C=O stretch (COOH)
5	1550–1650	N–H bend
6	1540–1650	C=O asymmetric stretch (COO^-)
7	1360–1450	C=O symmetric stretch (COO^-)

Some IR band positions are available from http://www.infrared.als.lbl.gov/content/web-links/60-ir-band-positions.

The FTIR method using reflectance sampling techniques allowed a straightforward measurement of salts in their native state (dry/wet powder or single crystals), requiring minimum sample amount for analysis (< 1 mg), eliminating the need for sample pre-treatment, minimizing the possibility of phase transformation during sampling and giving a distinctive pattern for each salt form. Therefore, it served as a fast, direct and reliable tool to confirm salt formation and was especially useful in routine phase identification of metastable forms and detection of potential phase transformations.

3.5. Thermal stability analysis (TGA and DSC) and hydrate characterization

TGA curves of 1:1 and 2:1 salt pairs are shown in Fig. 8. As expected, no weight loss was observed on melting 1:1 anhydrous salt pairs; further heating led to 40% weight loss at higher temperature (140–240 °C) due to decomposition of the salts, Fig. 8a and b. The 2:1_MH salt pair exhibited constant weight loss (4.7% for 2:1 LL_MH and 3.6% for 2:1 LD_MH) between 60 and 110 °C, Fig. 8c and d, which attributed to loss of water from the crystal lattice. The dehydration characteristics of these 2:1 salts are somewhat different: a clear single dehydration step was observed for 2:1 LD_MH, while the dehydration step(s) for 2:1 LL_MH is less apparent, shown as a gradual weight loss on dehydration. Both dehydration steps were followed by a major 60% weight loss as decomposition/volatilisation of the anhydrous solid occurred on melting. Water contents of 2:1 MH salts from TGA data are in good agreement with the theoretical value (3.6% for 1 molecule of water per molecule of salt): the weight loss from dehydration of 2:1 LL_MH and 2:1 LD_MH is 4.7% and 3.6%, respectively; therefore both hydrates should have MH composition, in agreement with elemental analysis (Table 2). However, there is an uncertainty about the water content in 2:1 LL hydrate because TGA data could suggest the formation of a sesquihydrate. The determination of an accurate weight loss value corresponding to dehydration from TGA is ambiguous due to the gradual loss of water on dehydration rather than a characteristic sharp dehydration step.

The thermal features of salts were better revealed from DSC thermograms, also shown in Fig. 8. DSC data of both 1:1 anhydrous salts show a sharp melting endotherm: ~126 °C for 1:1 LL (ΔH=127 J/g) and ~103 °C for 1:1 LD salt (ΔH=83 J/g). In the case of MH forms, similar thermal behavior was observed for LL and LD salts with three endothermic events around 60–110 °C, 120–170 °C and 140–220 °C. The first broad endotherm is attributed to dehydration and correlates well with TGA data. The second sharp melting endotherm (peaking at ~163 °C for 2:1 LL_MH, ~158 °C for 2:1 LD_MH) overlapped with the third broad endotherm, indicating that decomposition commenced on melting, which was further confirmed by the pattern of weight loss over this temperature range by TGA.

Strictly speaking, the melting behavior observed for 2:1 MH corresponds to that of 2:1 anhydrous form and should be related only to the thermal stability of that form. Thus, both anhydrous LL forms (1:1 LL and 2:1 LL) showed higher melting temperature than their LD analogs (1:1 LD and 2:1 LD), indicating their greater thermal stability and hence relatively lower aqueous solubility, suggesting that, in principle, LL anhydrous forms could be separated from LD anhydrous forms by crystallization due to their different stability and solubility. To prove such a suggestion, however, complete solubility data of both forms in water is needed. Our preliminary solubility tests suggested very high solubility for both 1:1 LL and 1:1 LD salts. Actually, because of the high concentration of the aqueous saturated solution, separation of the crystallizing solid phase from the liquid phase was not feasible due to the formation of a highly-viscous solution/gel before the precipitation of salts. For 2:1 anhydrous salts, difficulties arose due to the stability of such forms in water:solution-mediated transformations 2:1 LL→2:1 LL_MH and 2:1 LD→2:1 LD_TH were observed to take place during the solubility measurements. Searches for alternative techniques to measure aqueous solubility and suitable experimental conditions to avoid phase transformation are underway.

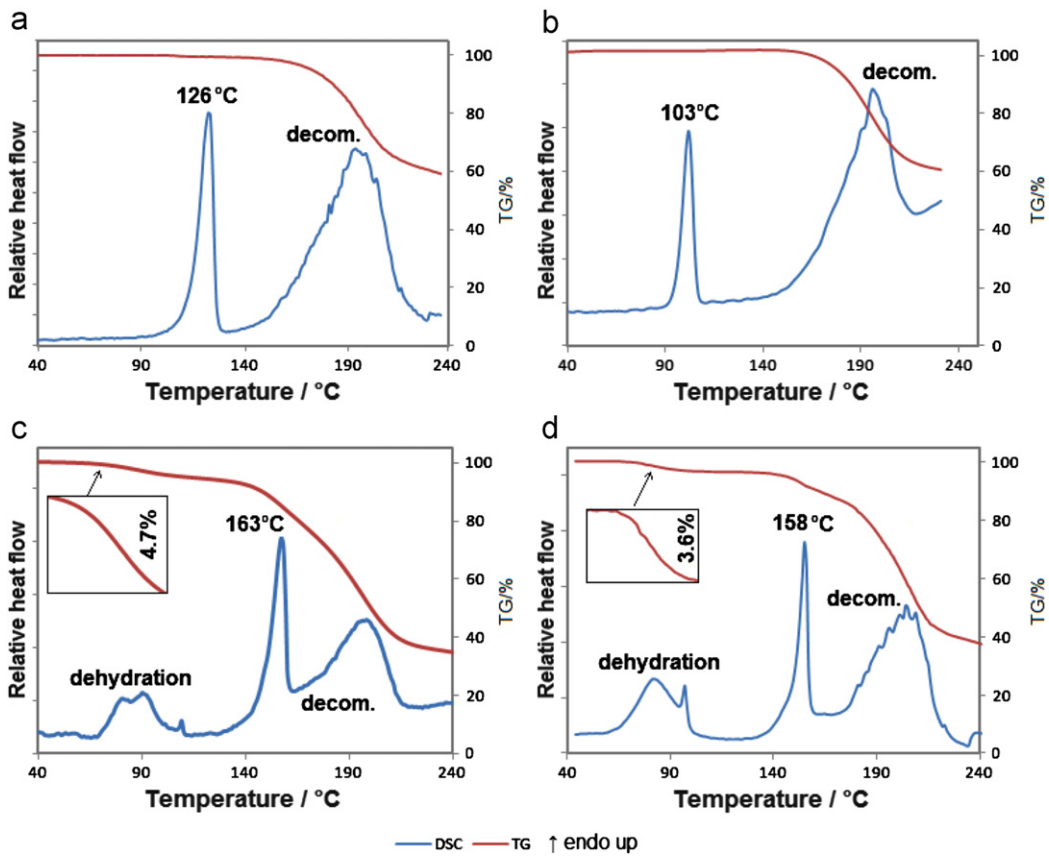

Fig. 8. DSC and TGA curves of 1:1 and 2:1_MH salt pairs. (a) 1:1 LL, (b) 1:1 LD, (c) 2:1 LL_MH and (d) 2:1 LD_MH

The solid forms of L-Eph salts showed much higher melting point (100–161 °C) than its free base (~37 °C, $\Delta T > 60$ °C). The problems with a low melting point for drug forms are obvious: plastic deformation and formation of localized welds normally lead to bulk aggregation and caking, these affect flow, compression and dissolution properties. The increase in melting point of drug forms is usually accompanied by enhanced thermodynamic stability, easier processing conditions and improved relative compatibility with formulation excipients (Li Wan Po and Mroso, 1984). The consideration of melting point is always one of the key properties in assessing the desirability of drug forms, and usually a high melting point form is preferred (exceptions occur when solubility is dramatically decreased by the increase of melting point).

3.6. Moisture-dependant stability and phase transitions of solid salts

One of the key parameters in drug development is the hygroscopic nature of the drug forms, and soluble polar salts have a propensity to be hygroscopic. For this reason, all 1:1, 2:1 and 2:1 MH salt forms were subjected to a gravimetric moisture sorption study at 25 °C, Fig. 9.

Both 1:1 anhydrous salts are not hygroscopic at RH $\leq$70%, with a water uptake $<$2% (Fig. 9a and b). However, at higher RH, both salts absorbed a large amount of moisture, eventually leading to deliquescence at $>$90% RH. The desorption isotherm of 1:1 LD salt showed partial recrystallization at decreasing RH with 8% water residue at 0% RH, and the formation of highly viscous solution.

Neither 2:1 LL hydrous nor anhydrous salts are hygroscopic at RH $\leq$80%, with a water uptake $<$1% (Fig. 9c and d). With increasing RH, both salts gradually absorbed more moisture up to ~8% and ~25% water content at 95% RH in hydrate and anhydrate form, respectively. In the second sorption–desorption isotherm, 2:1 LL_MH absorbed less water, ~4% at 95% RH, due to the insufficient exposure time compared to the first cycle: ~20 h at 95% RH in cycle 1, and ~7 h at 95% RH in cycle 2 (the maximum time set for each step is 20 h). The transformation between MH and anhydrous forms was difficult for RH control; full dehydration of MH to give anhydrous form was observed only by heating MH to 110 °C. The DVS analysis indicated both 2:1 LL salts were non-hygroscopic, and could be stored under ambient environment without phase interconversion.

Two sorption–desorption isotherms of 2:1 LD_MH (Fig. 9e) showed that a mass uptake of ~7% was observed at 80% RH, and a further ~20% water uptake was obtained at 95% RH. Similar dehydration behavior was seen on desorption: 7.3–7.9% water remained at 80–50% RH and eventually 0% below 40% RH. The character of the soption–desorption isotherms revealed the existence of another kinetically stable hydrate form, 2:1 LD_TH (theoretical value 7.46%), which was stable only at high RH and readily transformed to MH under ambient conditions. Sharp steps and strong hysteresis between phase transitions indicated that both MH and TH forms are stoichiometric hydrates, they could also be separated and stored under suitable conditions. 2:1 LD_MH was particularly stable at low RH; no dehydration was observed after a couple of hours at 0% RH and full dehydration to give anhydrous form was achieved only by heating MH to 110 °C. This was further supported by the DVS analysis of 2:1 LD anhydrous salt under various RH (Fig. 9f): transformation to MH was seen at 70% RH (3.84% water content, theoretical expected value 3.87%), and to TH at 80% RH (11.5% water uptake, theoretical value 11.62%).

The hygroscopic character depends on the nature of the solid and the exposed surfaces (the balance of hydrophobic and hydrophilic faces) and consequently stoichiometry and chirality

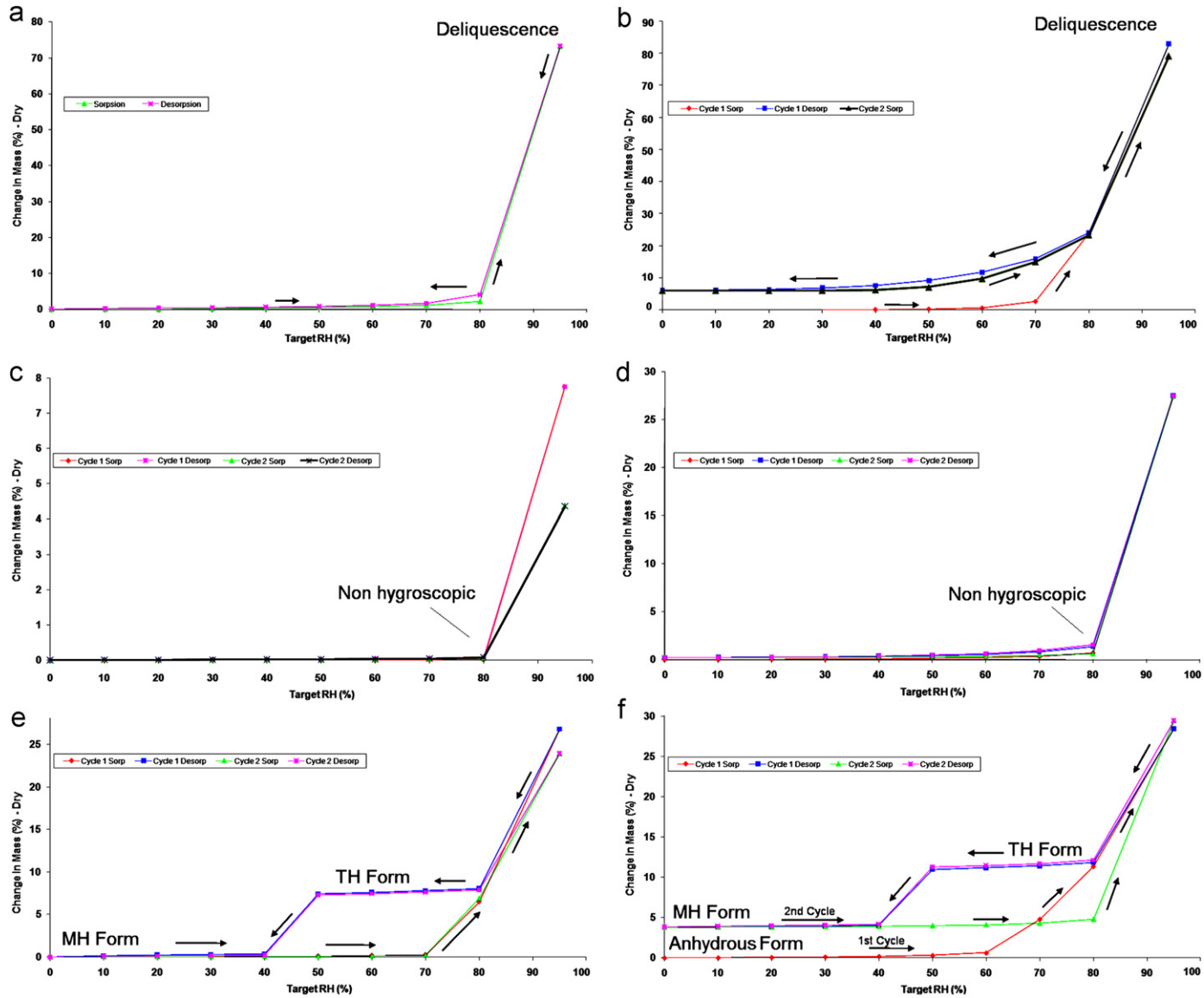

Fig. 9. DVS isotherms of (a) 1:1 LL, (b) 1:1 LD, (c) 2:1 LL_MH, (d) 2:1 LL, (e) 2:1 LD_MH and (f) 2:1 LD salts.

variation in the salt forms have unavoidable impact on their hygroscopicity. The moisture-dependant phase tranformations: anhydrate→MH→TH→MH indicated that similar phenomena could occur during drug formulation and wet processing steps (e.g. granulation and coating), or even during transport and storage where humidity and temperature may vary.

4. Conclusions

So far, seven different solid forms of L-Eph salts (1:1 and 2:1 stoichiometry, anhydrates, MH, TH) have been prepared by solution crystallization, dry/wet grinding crystallization and RH controlled crystallization; only one salt, 1:1 LL, was previously known (Collier et al., 2006). The stability, ionization state, melting point, thermal transformation and hygroscopicity of the seven salts were characterized and a variety of structure related properties of the various salt forms were observed. Water, used as the only solvent in this system, played an indispensable role in salt formation and solid state transformations of 2:1 salts.

In food and pharmaceutical industries, salt formation provides a potential method to fine-tune drug properties and their biological characteristics without changing its chemical structure. The selection of an advantageous salt form depends on specific requirements of crystallinity, stability, processability, solubility, dissolution rate, hygroscopicity and bioavailability (Gould, 1986), as well as cost and availability of the acid. Therefore, a systematic, detailed investigation of salt formation and characterization is essential in assessment of suitable salt forms. Our study provides an example of a simple system that consists of 7 different solid forms with variable physicochemical properties. The formation of various salts by a simple acid–base reaction, reported here, should not be an isolated case. It would be interesting to apply a similar approach to explore other systems (dibasic acids) where a wide spectrum of salt forms may exist.

The synthesized diastereomeric L-Eph salts are considered as intermediate products during chiral resolution of the acid, their structure and physiochemical properties are known to be crucial in successful separation of the enantiomeric mixtures. The inevitable differences found in stoichiometry, stability, solubility and hydrate formation could lead to complications in chiral

resolution: it is not possible to predict which salt form, or hydrate will precipitate first from a racemic mixture as the solution is far beyond the ideal situation where only a single salt pair should exist.

Previous studies on the feasibility of chiral resolution based on the phase diagram of polymorphic malic acid showed it is potentially complex since partial solid solutions form (Kaemmerer et al., 2009).

In this study, we demonstrated the formation of 7 different salts in a simple L-Eph–Malic acid–H_2O system, without an attempt at exhaustive polymorph/solvate screening. Prediction of resolution conditions and efficiency is likely to be difficult. First, the ternary phase diagram will, inevitably, be complex. Second, it is possible that salts at stoichiometry different from 1:1 and 2:1 may also crystallize. We have no information on this at the moment.

With the rapid development of computational techniques and methods, attempts to correlate crystal structures with their performance in chiral resolution process were proposed (Faigl et al., 1990; Leusen et al., 1991, 1992). This strategy was demonstrated by Price (e.g. Karamertzanis et al., 2007) in qualitatively predicting the resolution efficiency of (R)-1-phenylethylammonium performed on 2-phenylacetate derivatives. The application of this model to other systems is, however, challenging and needs to be validated by experimental evidence. Our XRD and IR studies of L-Eph–Malic acid–H_2O salt pairs show crystal lattice differences between each form and provide another potential system to test this model. Determination of the crystal structures of the salt pairs, especially the position of H atoms and the variation in H-bonding motifs, is essential; further work is in progress.

Acknowledgments

This work was carried out with financial support from the Engineering Physical Science Research Council (EPSRC, EP/F006721/1) and EPSRC Engineering Instrument Pool (Hirox 3D Digital Microscope and Diamond DSC). The authors thank Prof. Roger Davey and Mr. Kevin Back for generous provision and help with DVS measurements. Thanks are also given to Prof. Sally Price, Prof. Derek Tocher, Dr. Panagiotis Karamertzanis, Dr. Jeremy Cockcroft, Dr. Doris Braun and Mr. Miguel Ardid Candel for useful discussions.

References

Aakeroy, C.B., Fasulo, M.E., Desper, J., 2007. Cocrystal or salt: does it really matter? Mol. Pharm. 4 (3), 317–322.

Abourashed, E.A., El-Alfy, A.T., Khan, I.A., Walker, L., 2003. Ephedra in perspective—a current review. Phytother. Res. 17, 703–712.

Anandamanoharan, P.R., Cains, P.W., Jones, A.G., 2006. Separability of diastereomeric salt pairs of 1-phenylethylamine with enantiomeric 2-substituted phenylacetic acids by fractional crystallization, and its relation to physical and phase properties. Tetrahedron: Asymmetry 17, 1867–1874.

Black, S.N., Collier, E.A., Davey, R.J., Roberts, R.J., 2007. Structure, solubility, screening, and synthesis of molecular salts. J. Pharm. Sci. 96 (5), 1053–1068.

Chadwick, K., Davey, R.J., Cross, W., 2007. How does grinding produce co-crystals? Insight from the case of benzophenone and diphenylamine. Chem. Commun. 9, 732–734.

Childs, S.L., Stahly, G.P., Park, A., 2007. The salt–cocrystal continuum: the influence of crystal structure on ionization state. Mol. Pharm. 4 (3), 323–338.

Collier, E.A., Davey, R.J., Black, S.N., Robert, R.J., 2006. 17 salts of ephedrine: crystal structures and packing analysis. Acta Crystallogr. B 62, 498–505.

Cooke, C.L., Davey, R.J., Black, S., Muryn, C., Pritchard, R.G., 2010. Binary and ternary phase diagrams as routes to salt discovery: ephedrine and pimelic acid. Cryst. Growth Des. 10 (12), 5270–5278.

Faigl, F., Simon, K., Lopata, A., Kozsda, E., Hargitai, R., Czugler, M., Acs, M., Fogassy, E., 1990. A combined DSC, X-ray diffraction, and molecular modelling study of chiral discrimination in the purification of enantiomeric mixtures of cis-permethrinic acid. J. Chem. Soc. Perkin Trans. 2, 57–63.

Gould, P.L., 1986. Salt selection for basic drugs. Int. J. Pharm. 33, 201–217.

Jacques, J., Collet, A., Wilen, S.H., 1981. Enantiomers, Racemates and Resolutions. John Wiley & Sons, New York.

Kaemmerer, H., Lorenz, H., Black, S.N., Seidel-Morgenstern, A., 2009. Study of system thermodynamics and the feasibility of chiral resolution of the polymorphic system of malic acid enantiomers and its partial solid solutions. Cryst. Growth Des. 9, 1851–1862.

Karamertzanis, P.G., Anandamanoharan, P.R., Fernandes, P., Cains, P.W., Vickers, M., Tocher, D.A., Florence, A.J., Price, S.L., 2007. Toward the computational design of diastereomeric resolving agents: an experimental and computational study of 1-phenylethylammonium-2-phenylacetate derivatives. J. Phys. Chem. B 111, 5326–5336.

Kozma, D., 2001. CRC Handbook of Optical Resolution via Diastereomeric Salt Formation. CRC Press, Boca Raton.

Leusen, F.J.J., Bruins Slot, H.J., Noordik, J.H., van der Haest, A.D., Wynberg, H., Bruggink, H., 1991. Towards a rational design of resolving agents. Part III. Structural study of two pairs of diastereomeric salts of ephedrine and a cyclic phosphoric acid. Rec. Trav. Chim. Pays-Bas 110 (1), 13–18.

Leusen, F.J.J., Bruins Slot, H.J., Noordik, J.H., van der Haest, A.D., Wynberg, H., Bruggink, H., 1992. Towards a rational design of resolving agents. Part IV. Crystal packing analyses and molecular mechanics calculations for five pairs of diastereomeric salts of ephedrine and a cyclic phosphoric acid. Rec. Trav. Chim. Pays-Bas 111 (3), 111–118.

Li Wan Po, A., Mroso, P.V., 1984. Drug–drug incompatibility in the solid state: kinetic interpretation, modelling and prediction. Int. J. Pharm. 18, 287–298.

Shirley, R., 1980. Block, S., Hubbard, C.R. (Eds.), Accuracy in Powder Diffraction. NBS Spec. Publ. 567, pp. 361–382.

Spectral Database for Organic Compounds SDBS, 2011. Web: 〈http://riodb01.ibase.aist.go.jp/sdbs/〉 (National Institute of Advanced Industrial Science and Technology).

Stahl, P.H., Wermuth, C.G., 2002. Handbook of Pharmaceutical Salts: Properties, Selection, and Use. Wiley-VCH, Weinheim.

Van de Streek, J., 2007. All series of multiple solvates (including hydrates) from the Cambridge Structural Database. CrystEngComm 9, 350–352.

Vermeulen, N.P.E., te Koppele, J.M., 1993. Stereoselective biotransformation: toxicological consequences and implications. In: Wainer, W.I. (Ed.), Drug Stereochemistry: Analytical Methods and Pharmacology, 2nd ed. , Marcel Dekker, Inc., NewYork, pp. 245–280.

Wu, H., Reeves-Mclaren, N., Jones, S., Ristic, R.I., Fairclough, J.P.A., West, A.R., 2010a. Phase transformations of glutamic acid and its decomposition products. Cryst. Growth Des. 10, 988–994.

Wu, H., Reeves-Mclaren, N., Pokorny, J., Yarwood, J., West, A.R., 2010b. Polymorphism, phase transitions, and thermal stability of L-pyroglutamic acid. Cryst. Growth Des. 10, 3141–3148.

Wu, H., West, A.R., 2011. Thermally-induced homogeneous racemization, polymorphism, and crystallization of pyroglutamic acid. Cryst. Growth Des. 11, 3366–3374.